

A large population of recently quenched red-sequence dwarf galaxies in the outskirts of the Coma cluster[★]

Russell J. Smith,^{1†} Ronald O. Marzke,² Ann E. Hornschemeier,³ Terry J. Bridges,⁴ Michael J. Hudson,⁵ Neal A. Miller,⁶ John R. Lucey,¹ Gerardo A. Vázquez^{6,7} and David Carter⁸

¹*Department of Physics, University of Durham, Durham DH1 3LE*

²*Department of Physics and Astronomy, San Francisco State University, San Francisco, CA 94132, USA*

³*NASA Goddard Space Flight Center, Code 662.0, Greenbelt, MD 20771, USA*

⁴*Department of Physics, Queen's University, Kingston, Ontario K7L 3N6, Canada*

⁵*Department of Physics and Astronomy, University of Waterloo, 200 University Avenue West, Waterloo, Ontario N2L 3G1, Canada*

⁶*Department of Physics and Astronomy, Johns Hopkins University, 3400 North Charles Street, Baltimore, MD 21218, USA*

⁷*Department of Physics, Salisbury University, 1101 Camden Avenue, Salisbury, MD 21801, USA*

⁸*Astrophysics Research Institute, Liverpool John Moores University, Twelve Quays House, Egerton Wharf, Birkenhead CH41 1LD*

Accepted 2008 February 29. Received 2008 February 28; in original form 2008 February 4

ABSTRACT

We analyse the stellar populations of 75 red-sequence dwarf galaxies in the Coma cluster, based on high signal-to-noise ratio spectroscopy from the 6.5-m MMT. The sample covers a luminosity range 3–4 mag below M^* , in the cluster core and in a field centred 1° to the south-west. We find a strong dependence of the absorption-line strengths with location in the cluster. Galaxies further from the cluster centre have stronger Balmer lines than inner-field galaxies of the same luminosity. The magnesium lines are weaker at large radius, while the iron lines are not correlated with radius. Converting the line strengths into estimates of stellar age, metallicity and abundance ratios, we find the gradients are driven by variations in age ($>6\sigma$ significance) and in the iron abundance Fe/H ($\sim 2.7\sigma$ significance). The light element (Mg, C, N, Ca) abundances are almost independent of radius. At radius of $0.4\text{--}1.3$ ($\sim 0.3\text{--}1.0$ times the virial radius), dwarf galaxies have ages ~ 3.8 Gyr on average, compared to ~ 6 Gyr near the cluster centre. The outer dwarfs are also ~ 50 per cent more iron-enriched, at given luminosity. Our results confirm earlier indications that the ages of red-sequence galaxies depend on location within clusters, and in Coma in particular. The very strong trends found here suggest that dwarf galaxies are especially susceptible to environmental ‘quenching’, and/or that the south-west part of Coma is particularly a clear example of recent quenching in an infalling subcluster.

Key words: galaxies: clusters: individual: Coma – galaxies: dwarf.

1 INTRODUCTION

Galaxies in rich clusters are subject to a range of environmental processes (stripping, suffocation, harassment, tides), which are absent, or at least less efficient, in the field and in poor groups. The role of these effects in ‘quenching’ star formation in cluster galaxies has been widely discussed based on instantaneous star formation tracers such as H α emission. For example, the fraction of star-forming galaxies is suppressed out to ~ 3 times the virial radius R_{200}

(e.g. Lewis et al. 2002). To trace the history of environment-driven quenching in today’s galaxy clusters, high-quality spectroscopy is needed to determine the final epoch of star formation in now passive galaxies.

A number of works have claimed to observe significant variation in absorption-line strengths of galaxies, as a function of radius in clusters (e.g. Guzmán et al. 1992; Carter et al. 2002; Smith et al. 2006). These trends have been interpreted as a radial gradient in average stellar age. Smith et al. note evidence that dwarfs may exhibit stronger radial dependences than the more massive galaxies, as expected if the efficiency of the quenching process depends on the depth of the potential well-binding the gas reservoirs.

In this Letter, we provide further evidence for strong cluster-centric gradients in age for dwarf galaxies (median $M_r \approx -17.5$)

[★]Observations reported here were obtained at the MMT Observatory, a joint facility of the University of Arizona and the Smithsonian Institution.

†E-mail: russell.smith@durham.ac.uk

in Coma, using new spectroscopic data from the 6.5-m MMT. A comprehensive analysis of the stellar populations will appear in a future paper (Smith et al., in preparation). For luminosity and distance calculations, we adopt a distance to Coma of 100 Mpc.

2 OBSERVATIONS AND PARAMETER MEASUREMENTS

High signal-to-noise ratio (S/N) spectra were obtained using the Hectospec fibre-fed spectrograph (Fabricant et al. 2005) on the MMT, in 2007 February–April. The instrument deploys 300 fibres over a 1° diameter field of view (corresponding to 1.75 Mpc at Coma); the fibre diameter is 1.5 arcsec (0.7 kpc). Two fields were observed, one centred on the cluster core and an outer field to the south-west (Fig. 1). The choice of the south-west field was motivated by available supporting data, and influenced by the work of Caldwell et al. (1993) who reported a high fraction of Balmer strong galaxies in this region.

Our observations were made in parallel with an extensive redshift survey of the cluster (Hornschemeier et al., in preparation). To study the stellar populations of dwarf galaxies, we observed 79 known cluster members with luminosities 3–4 mag below M^* , plus 10 brighter galaxies for overlap with previous studies (e.g. Sánchez-Blázquez et al. 2006). The target galaxies were selected to lie close to the red sequence of non-star-forming galaxies (Fig. 2). The 270 line mm^{-1} grating was used, resulting in a wide wavelength coverage (3700–9000 Å) at a spectral resolution of 4.5 Å, full width at half-maximum. The median total integration time for the faint

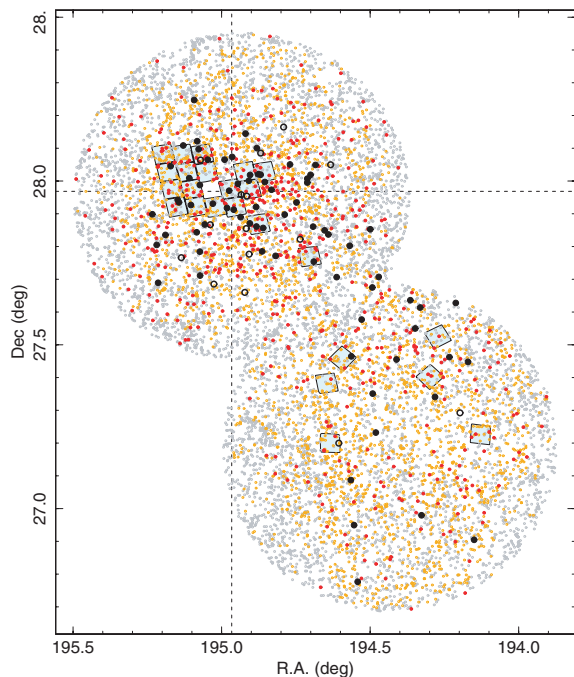


Figure 1. Sky distribution of the line-strength sample (black). The filled points are galaxies used in the fits of Section 3. Open symbols are either bright ($M_r < -19$) comparison galaxies, have emission lines, or no measured age. Small points show other SDSS galaxies within the Hectospec survey region in red (confirmed members), yellow (confirmed background galaxies) or grey (no redshift information). The redshifts are from our Hectospec survey and literature sources. Pale-blue squares indicate the regions covered by *Hubble Space Telescope* imaging from the Coma ACS Treasury Survey (Carter et al. 2008). Cross-hairs show the adopted cluster centre, midway between the two central cD galaxies.

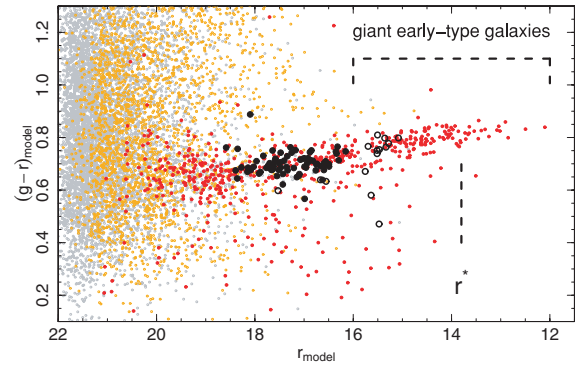


Figure 2. The $g - r$ colour magnitude diagram for the galaxies in Fig. 1, from SDSS photometry. For comparison, we note the position of the luminosity function break, r^* , and the magnitude range for ‘giant’ early-type galaxies, having velocity dispersions $\sigma \gtrsim 75 \text{ km s}^{-1}$. The symbols are as in Fig. 1.

galaxies was ~ 7 h, yielding typical S/N of $\sim 40 \text{ \AA}^{-1}$ (at $\sim 5000 \text{ \AA}$). The brighter galaxies were observed for 0.7–2.0 h. Relative flux calibration was imposed using F stars with photometry from Sloan Digital Sky Survey (SDSS, Adelman-McCarthy et al. 2007), observed simultaneously with the galaxies in each configuration. The data were reduced using HSRED, an automated IDL package based on the SDSS pipeline, provided by Richard Cool.

Analysis of the one-dimensional spectra, including combination of multiple exposures and measurements of emission and absorption lines, followed methods used by Smith, Lucey & Hudson (2007). Three galaxies with $\text{H}\alpha$ in emission (equivalent width $\gtrsim 20 \text{ \AA}$) were removed from the sample. No other galaxies have emission above $\sim 0.5 \text{ \AA}$ after removing the stellar continuum. Absorption-line indices were measured and corrected to the Lick resolution, but not transformed to the Lick ‘system’, since we will use models based on flux-calibrated spectral libraries. Comparisons with the index measurements of Sánchez-Blázquez et al. (2006) show excellent agreement for eight galaxies in common (e.g. HgF offset $0.1 \pm 0.1 \text{ \AA}$ with rms scatter 0.2 \AA).

Line-strength measurements can be transformed into estimates of stellar population age and element abundances, through comparison with population synthesis models. In this Letter, we analyse the absorption-line measurements with reference to new stellar population models by Schiavon (2007). Advantages of this model set include its basis in a flux-calibrated stellar library, individually variable Mg, C, N and Ca abundances at fixed Fe/H, and a publicly available code EZ-AGES for estimating parameters from measured indices (Graves & Schiavon 2008).

The EZ-AGES code performs an iterative ‘sequential’ grid inversion, finding abundance ratios which yield consistent age and metallicity estimates across a range of index–index diagrams. A full description of the method is given by Graves & Schiavon (2008), while a summary can be found in Schiavon (2007). In our implementation, an initial estimate of age and Fe/H is made using Hbeta and the iron indices Fe5270 and Fe5335 assuming solar-scaled abundances. The Mg/Fe ratio is adjusted to yield the same metallicity and age from Hbeta and Mg5177. Similarly, C/Fe is obtained using the Fe4668 index (which is heavily influenced by the C abundance). With C/Fe in hand, the N/Fe abundance is adjusted for consistency with the measured CN2. Finally, Ca/Fe is obtained from Ca4227. The procedure is iterated, deriving a new age and metallicity estimate from the updated abundance pattern in each step. Once the final abundances

are obtained, ages are estimated using the higher order Balmer indices H δ F and H γ F, as well as using H β . Errors are determined from Monte Carlo simulations.

3 RADIAL TRENDS

In this section, we examine the evidence for trends in our sample of Coma dwarfs, both at the level of observed indices and also using the derived ages and metallicities. Because the stellar populations of red galaxies follow strong scaling relations with the mass or luminosity (e.g. Smith et al. 2007), we analyse the residuals from the index–luminosity (and age–luminosity relations, etc.), rather than the index data themselves. Thus, we are comparing the inner and outer galaxy population at fixed luminosity. (In fact, there is no correlation of luminosity with radius within our galaxy sample, so similar results would be obtained without this control.) We exclude the brighter comparison galaxies (with $r < 16$), and one object for which EZ-AGES failed to converge, leaving 75 galaxies in the fits. All galaxies are assigned equal weight in the fits, since the scatter is primarily intrinsic and the measurement errors similar for all points.

The residual index–radius relations are shown in Fig. 3, for the nine indices which enter into our analysis with EZ-AGES. Strong positive correlations are observed in all of the Balmer indices: H β (5σ), H γ F (4σ) and H δ F (4σ). Negative, but generally less significant, trends are recovered for most of the metal indices dominated by light elements: CN2 (3σ), Mgb5177 (3σ) and Ca4227 (2σ). Finally, the carbon-dominated index Fe4668 and iron-dominated Fe5270 and Fe5335 show no significant correlation.

Fig. 4 presents the equivalent relations for the derived age (estimated from each Balmer index, and the average age), the metallicity Fe/H and the four light-element abundance ratios (Mg/Fe, C/Fe, N/Fe and Ca/Fe). We find a strong (5σ) correlation towards younger ages at larger radii, whether measured with H β , H γ F or H δ F. The

size of the effect is consistent between age indicators. Using the average of the three ages obtained for each galaxy, the age–radius correlation is significant at the 6.5σ level, and its slope implies a factor of 2 change in age, per degree in radius. The median age for the galaxies beyond 0.4 from the centre is 3.8 Gyr, corresponding to their star formation being quenched at $z \lesssim 0.3$ (Fig. 5).

The iron abundance, Fe/H shows a significant (2.7σ) correlation $0.20 \pm 0.07 \text{ dex deg}^{-1}$, with higher metallicity at larger radius. (Note that the absence of a trend in Fe5270 e.g. reflects the compensating effect of the age and Fe/H gradients.) The Mg/Fe abundance ratio is significantly smaller at large radius by $0.13 \pm 0.04 \text{ dex deg}^{-1}$. Note that the magnesium abundance $[\text{Mg}/\text{H}] = [\text{Mg}/\text{Fe}] + [\text{Fe}/\text{H}]$ is consistent with being independent of location in the cluster; thus, the variation in $[\text{Mg}/\text{Fe}]$ is driven by the greater iron abundance in the outer galaxies, not by lower magnesium. The other abundance ratios are also smaller at larger radius, but with lower significance levels, $\sim 2\sigma$. The abundances N/H and Ca/H are, like Mg/H, consistent with no radial variation, while C/H may be marginally increasing with radius (2σ).

Magnesium is produced mainly by Type II supernovae, while iron is released primarily by Type Ia supernovae, which are delayed with respect to star formation. Therefore, the smaller Mg/Fe (and larger Fe/H) at large radius suggest the outer galaxies had extended star-formation histories prior to their quenching. In this scenario, it is qualitatively expected that a trend to younger ages would be accompanied by a trend towards lower Mg/Fe. Quantitatively, however, galactic chemical evolution models are required to determine what star formation and enrichment histories could reproduce the observed behaviour.

Finally, we note there is a significant radial colour correlation for the sample, with a slope $-0.05 \pm 0.01 \text{ mag deg}^{-1}$ in $g - r$ (bluer colour at larger radius). A small shift, with the same sense, was previously noted by Terlevich, Caldwell & Bower (2001) and

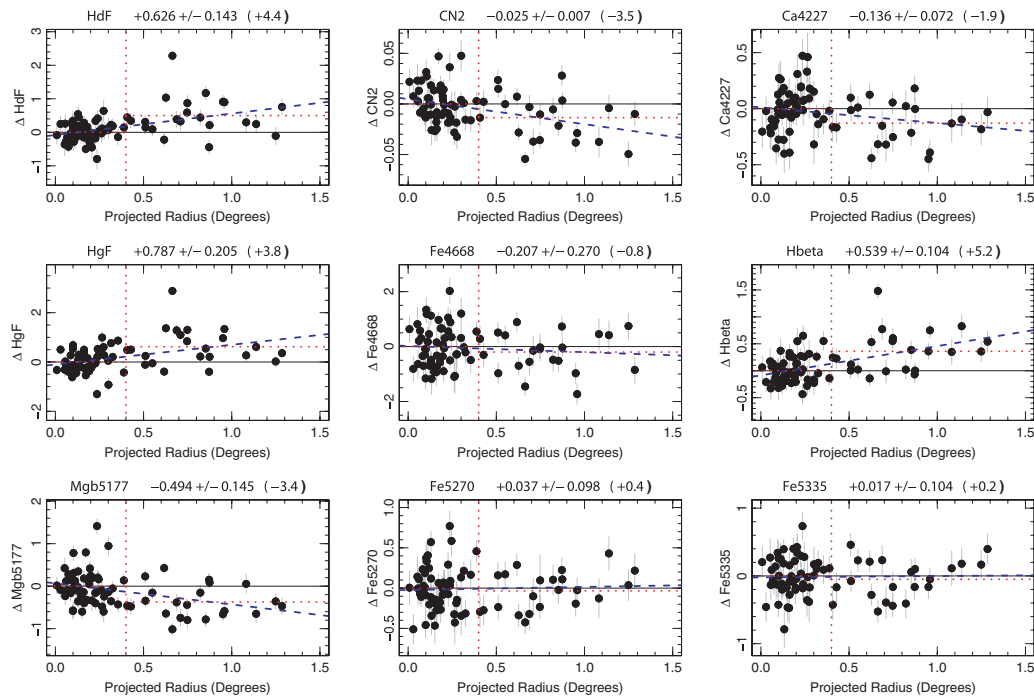


Figure 3. Radial trends in the index residuals. The title bar for each index I gives the coefficient of projected radius R_{proj} in a bivariate fit of the form $I = a_0 + a_1 M_r + a_2 R_{\text{proj}}$. The significance of the radial trend is given in parentheses in units of the standard error. The red dotted lines show median residuals inside and outside 0.4, while the dashed blue line shows an unweighted fit to the residuals.

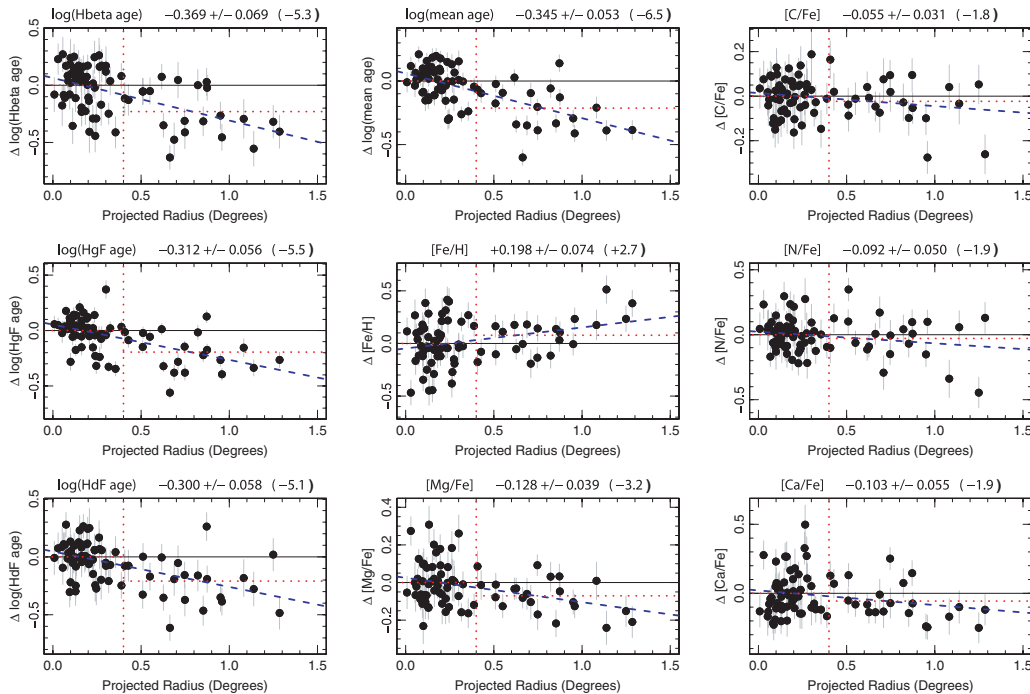


Figure 4. Radial trends in the stellar population parameters from EZ-AGES. The annotations are as in Fig. 3.

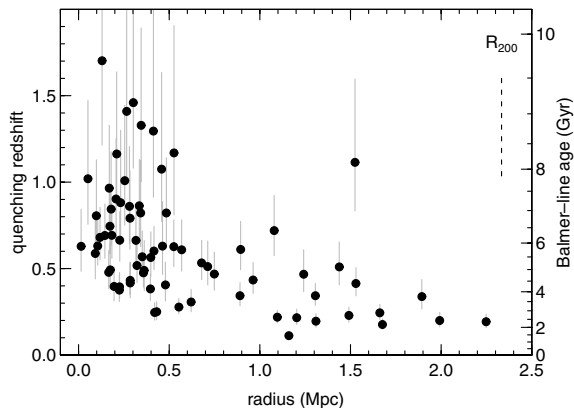


Figure 5. Quenching redshift, defined here as the redshift for which the look-back time is equal to the Balmer age, as a function of projected distance from the cluster centre. Although the most recent burst will generally be superposed on an older population, the Balmer age is strongly weighted towards the youngest stars present. If the mass fraction of the most recent burst is very small, the quenching redshifts plotted here are upper limits. The assumed cosmology has parameters $(\Omega_M, \Omega_\Lambda, h) = (0.3, 0.7, 0.7)$.

Carter et al. (2002). The galaxies beyond 0.4 have higher recession velocities by $340 \pm 220 \text{ km s}^{-1}$ than those in the core. Preliminary profile fits to SDSS images do not reveal significant radial trends in morphology.

4 DISCUSSION AND SUMMARY

Several authors have claimed to observe significant variation in absorption-line strengths as a function of radius in clusters, with much of this work focused on the Coma Cluster.

Caldwell et al. (1993) were the first to note a large fraction of galaxies with strong Balmer absorption in the south-west part of Coma. Their sample probed a smaller radial extent (out to ~ 50 arcmin) than our work, and was restricted to brighter galaxies ($r \lesssim 16$). Their result has driven other work in the south-west region, influencing the field placement of subsequent studies including the current one.

Carter et al. (2002) observed Coma galaxies over a wide-luminosity range, $r \sim 13\text{--}19$, in the cluster core and an outer field in the south-west. The fainter part of their sample corresponds to typical luminosities in our MMT work, and the radial extent is comparable. They found a significant radial decrease in the Mg_2 index at fixed luminosity, interpreting the result as a metallicity gradient, with lower metallicities in the cluster outskirts. However, their data for iron-dominated indices do not share the radial trend, while Hbeta is found to increase with radius. Taken together in fact, the results favour an interpretation in terms of age, rather than metallicity. Fig. 6 demonstrates a good agreement between Carter et al. (2002) and the present work, at the level of the index gradients. Our independent data, of much higher S/N, strongly confirm the earlier results for dwarfs in the south-west part of Coma.

For giant galaxies, outside of Coma, the situation appears quite different. Smith et al. (2006) analysed line strengths for ~ 3000 galaxies in ~ 90 clusters of the NOAO Fundamental Plane Survey (NFPS). The NFPS is dominated by M^* galaxies, i.e. with luminosities 15–40 times larger than our MMT sample. Smith et al. found stronger Balmer lines and weaker light-element features (Mgb5177, CN2, Fe4668) at larger distance from the cluster centres. The iron-dominated indices show no radial dependence. This pattern can be reproduced by variations in both the age and the α -element abundance ratio $[\alpha/\text{Fe}]$ (comparable to $[\text{Mg}/\text{Fe}]$), with no change in the overall metallicity $[\text{Z}/\text{H}]$ (comparable to $[\text{Mg}/\text{H}]$ here).

The NFPS index gradients are much shallower than those found here or by Carter et al. (Fig. 6). The relative pattern of gradients is

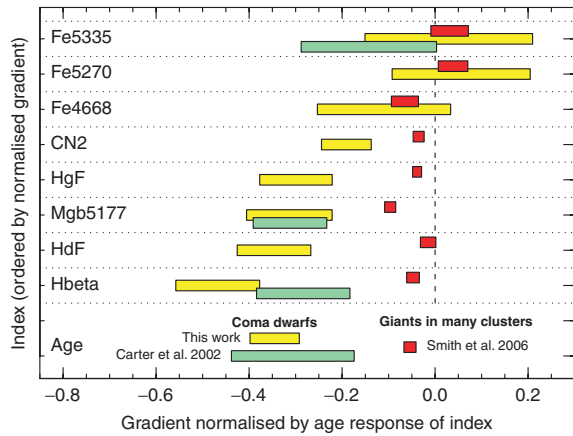


Figure 6. Comparison of our index gradient pattern (yellow) with previous work. For clarity, the results for each index have been normalized by its age response. Thus, if age was the only variable changing with radius, all indices should give the same gradient. Yellow boxes show the 1σ range from this work. For Carter et al. (2002, green), we compare their $\langle\text{Fe}\rangle$ with our Fe5335; their Mg2 gradient has been converted to an equivalent gradient in Mgb5177. For Smith et al. (2006, red), we have converted their gradients in R_{200} to degrees assuming $R_{200} \approx 80$ arcmin for Coma. The bottom row shows the age gradients derived for the three studies, including a new estimate for Carter et al., based on their published index gradients.

also different, with stronger gradients in the light-element indices than in the Balmer lines. This is reflected in the gradients of derived parameters: the Hectospec age gradient ($0.35 \text{ dex deg}^{-1}$) is seven times larger than the NFPS trend ($0.05 \text{ dex deg}^{-1}$), while the Mg/Fe trend ($0.12 \text{ dex deg}^{-1}$) is only a factor of 2.4 steeper than the NFPS trend in $[\alpha/\text{Fe}]$ ($0.04 \text{ dex deg}^{-1}$).

In conclusion, we have confirmed earlier indications that the spectra of faint red-sequence galaxies in Coma are correlated strongly with their distance from the cluster centre, at least towards the south-west. Our analysis, using the latest stellar population models, provides a clear interpretation of the observed trends as being primarily due to age. Since such strong radial trends are not seen, in general, for giant galaxies in clusters, a key question is whether the difference arises only from the different luminosity ranges, or whether the south-west region of Coma is unrepresentative. If the latter, we may be observing the descendants of star-bursting galaxies in cluster-

feeding filaments at $z \sim 0.2\text{--}0.3$ (e.g. Fadda et al. 2008). Future work must test whether dwarfs in other clusters, or in other parts of the Coma cluster exhibit similarly strong cluster-centric correlations. As one hint that the effect may not be confined to this region, Michielsen et al. (2008) have observed a sample of 18 dwarf ellipticals in Virgo, and find only young (~ 2 Gyr) objects beyond a radius of ~ 1 Mpc, equivalent to ~ 0.6 at Coma. A definitive answer for Coma itself should result from an extension to our Hectospec programme, which will obtain data in more fields to provide a complete azimuthal coverage to a radius of 1.5 , or ~ 2.5 Mpc.

ACKNOWLEDGMENTS

RJS was supported by PPARC/STFC rolling grant PP/C501568/1. ROM is supported by NSF grant AST-0607866. We thank Jenny Graves and Ricardo Schiavon for advice in using EZ-AGES. We are grateful to Richard Cool for making HSRED publicly available (<http://mizar.as.arizona.edu/rcool/hsred>), and for advice on Hectospec data reduction.

REFERENCES

- Adelman-McCarthy J. K. et al., 2007, *ApJS*, 172, 634
 Caldwell N., Rose J. A., Sharples R. M., Ellis R. S., Bower R. G., 1993, *AJ*, 106, 473
 Carter D. et al., 2002, *ApJ*, 567, 772
 Carter D. et al., 2008, *ApJS*, in press (arXiv:0801.3745)
 Fabricant D. et al., 2005, *PASP*, 117, 1411
 Fadda D., Biviano A., Marleau F. R., Storrie-Lombardi L. J., Durret F., 2008, *ApJ*, L9
 Guzmán R., Lucey J. R., Carter D., Terlevich R. J., 1992, *MNRAS*, 257, 187
 Graves G. J., Schiavon R. P. 2008, *ApJ*, in press (arXiv:0803.1483)
 Lewis I. J. et al., 2002, *MNRAS*, 334, 673
 Michielsen D. et al., 2008, *MNRAS*, in press (arXiv:0712.2017)
 Sánchez-Blázquez P., Gorgas J., Cardiel N., González J. J., 2006, *A&A*, 457, 787
 Schiavon R. P., 2007, *ApJS*, 171, 146
 Smith R. J., Hudson M. J., Lucey J. R., Nelan J. E., Wegner G. A., 2006, *MNRAS*, 369, 1419
 Smith R. J., Lucey J. R., Hudson M. J., 2007, *MNRAS*, 381, 1035
 Terlevich A. I., Caldwell N., Bower R. G., 2001, *MNRAS*, 326, 1547

This paper has been typeset from a $\text{\TeX}/\text{\LaTeX}$ file prepared by the author.